Online-Journals.org

iJOE International Journal of Online and Biomedical Engineering

iJOE | eISSN: 2626-8493 | Vol. 20 No. 12 (2024) | OPEN ACCESS

https://doi.org/10.3991/ijoe.v20i12.49773

PAPER

Exploring the Impact of Motion Parameter Variations in Virtual Reality Content on Visually Induced Motion Sickness: An Electroencephalography Signal Analysis Approach

Galih Restu Fardian Suwandi[1](✉), Siti Nurul Khotimah[1], Freddy Haryanto[1], Suprijadi[2]

[1]Nuclear Physics and Biophysics Research Group, Department of Physics, Faculty of Mathematics and Natural Sciences, Institut Teknologi Bandung, Bandung, Indonesia

[2]Instrumentation and Computation Physics Research Group, Department of Physics, Faculty of Mathematics and Natural Sciences, Institut Teknologi Bandung, Bandung, Indonesia

galihrfs@itb.ac.id

ABSTRACT

The utilization of virtual reality (VR) technology has surged during the COVID-19 pandemic, leading to a diversification of its applications. However, one significant challenge associated with VR usage is visually induced motion sickness (VIMS). To address this issue, a study was conducted to investigate the impact of variations in physical motion parameters on VR content in relation to VIMS. The study employed electroencephalography (EEG) signal analysis to measure the level of VIMS experienced by users as the motion characteristics of the content became more intricate, potentially inducing circular vection sensations. The results revealed noteworthy changes in power spectral density values within the alpha and beta brain wave frequency ranges in specific brain areas, including the frontal, parietal, and central regions. Furthermore, an elevation in stress levels and cognitive load was observed through power ratio analysis. These findings, which have direct implications for the design and advancement of VR content, are crucial for establishing an evaluation system for VR technology, ultimately mitigating adverse effects on users.

KEYWORDS

electroencephalography (EEG), virtual reality (VR), visually induced motion sickness (VIMS), power spectral density

1 INTRODUCTION

Amidst the transformative effects of the COVID-19 pandemic, virtual reality (VR) technology has been rapidly evolving and proving to be a valuable solution. As we adapt to new ways of working, learning, and connecting, VR offers an immersive and interactive experience that bridges the physical distance between individuals.

Suwandi, G.R.F., Khotimah, S.N., Haryanto, F., Suprijadi. (2024). Exploring the Impact of Motion Parameter Variations in Virtual Reality Content on Visually Induced Motion Sickness: An Electroencephalography Signal Analysis Approach. *International Journal of Online and Biomedical Engineering (iJOE)*, 20(12), pp. 160–176. https://doi.org/10.3991/ijoe.v20i12.49773

Article submitted 2024-05-01. Revision uploaded 2024-06-18. Final acceptance 2024-06-19.

Its success in facilitating collaboration and overcoming barriers has made it a major focus of post-pandemic study and development [1], [2], [3].

Virtual reality technology has garnered significant attention across various fields, but amidst all the excitement, a pressing concern—VIMS—demands our attention. VIMS is a condition that affects some VR users, causing them to experience discomforting symptoms such as nausea, dizziness, and visual fatigue due to a disparity between the sensation of movement perceived by the brain and the sensory information received by the body [4]. This issue is increasingly worrisome as VR finds use in diverse areas such as entertainment, education, and therapy [5]. It is, therefore, crucial to investigate the root causes of VIMS and develop effective mitigation strategies to ensure a more comfortable and secure VR user experience [6], [7].

Researchers have been studying the phenomenon of VIMS, which can occur when using VR technology. They have developed theories and models of sensory conflict to explain the causes of this problem. One prominent theory is the sensory conflict theory proposed by Reason [8], which suggests that a mismatch between visual, vestibular, and somatosensory information can lead to VIMS symptoms. Fernandes and Feiner [9] further developed this theory by emphasizing the role of conflict between visual and vestibular information in causing discomfort during VR use. Additionally, Sharples and colleagues [10] proposed a sensory conflict model that considers sensory disturbances, visual instability, and fatigue to explain VIMS symptoms fully. Bos and Bles [11] also developed the VIMS model, highlighting the role of mismatches between the brain's sensory information and external sensory inputs. Understanding these theories and models is crucial for preventing and treating VIMS as VR technology develops.

Numerous studies have been conducted to identify, alleviate, and assess VIMS in virtual reality technology. One popular method is questionnaires, such as the simulator sickness questionnaire (SSQ), which gauges user discomfort levels following VR use [12]. While these surveys offer a subjective report of VIMS symptoms, relying solely on questionnaire-based approaches can be insufficient for a comprehensive understanding of this phenomenon. Thus, studied have turned to body response measurements, such as ECG, EDA, EGG, respiration, body temperature, EMG, EEG, etc. Among these modalities, EEG has emerged as the most promising since it can record brain electrical activity with high time resolution, identifying patterns of brain activity associated with VIMS symptoms [13], [14], [15]. EEG measurements can provide a deeper understanding of how the brain reacts to VR use, thus facilitating the development of more effective intervention strategies [16].

Although there has been a lot of study on EEG-based VIMS, it has not been linked much to the theory and model of VIMS itself. Various studies have been conducted to develop and refine VIMS theories and models from a psychology and neuroscience perspective. This study produced several characteristics of conditions that can trigger VIMS. VIMS trigger characteristics have various aspects of motion, video quality, and visualization quality. Analysis of the characteristics of VIMS triggers has not been studied further using the EEG modality. This provides an opportunity to study VIMS more comprehensively.

This study aims to investigate the manifestation of VIMS symptoms induced by VR viewing, which is contingent upon the VIMS theory and model. The physical parameters associated with these symptoms will be analyzed through EEG measurements, providing an in-depth comparison between the theoretical causes of VIMS and their EEG-based results. This study, conducted during the pandemic, is particularly timely

and relevant, as it addresses a significant challenge associated with VR usage, VIMS, and provides insights that can help in the design and advancement of VR content. For those interested in the latest advancements in VR technology and how it impacts different aspects of life, it is worth exploring its potential in this new era, which holds promising opportunities for the future.

2 METHODS

This study was conducted in four primary phases. The initial phase involves preparation, which encompasses participant selection and VR content preparation. Next comes data acquisition, followed by data processing that includes EEG measurements and questionnaires. Finally, the fourth and last stage entails data analysis.

2.1 Participants

For this study, we recruited 35 male participants between the ages of 19 and 26. To ensure their suitability for the study, each potential participant underwent a screening process that included the motion sickness susceptibility questionnaire (MSSQ), consultations with general practitioners, and in-depth interviews. The interviews were designed to gather comprehensive background information related to the study theme, such as experiences with VR technology, phobias, and familiarity with EEG. Subsequent interviews were conducted after the EEG recording to gain insight into the participants' experiences during the session [17], [18].

Furthermore, a set of health-related standards was applied, ensuring no eye diseases, past eye surgeries or injuries, neurological disorders, brain damage, ear issues, abnormalities, or surgeries, and no ongoing medication-dependent treatments were present. After the screening procedure, 31 individuals were qualified to participate in the data collection phase.

The implementation of the experiments was meticulously guided by the principles outlined in the Declaration of Helsinki, which sets the ethical standards for medical study involving human subjects, ensuring respect for participants' rights and well-being. Additionally, the study adhered to specific technical requirements for study ethics, ensuring that the experimental design, procedures, and data handling met rigorous ethical guidelines as referenced in [19]. Before the commencement of EEG recording, all participants were thoroughly informed about the study's nature, purpose, and potential risks. Each participant provided their voluntary agreement to participate by signing an informed consent form, which detailed their rights, the confidentiality of their data, and the option to withdraw from the study at any time without penalty. This process ensured that all participants were fully aware of the study's procedures and role, thereby upholding the highest standards of ethical study practices.

2.2 Experimental devices

The study utilizes the Neuron-Spectrum-63, a clinical EEG device with 19 + 2 EEG electrodes (A1 and A2 as references and 19 scalp electrodes). The electrodes

are named based on their positions on the scalp, representing each lobe: frontal (Fp1, Fp2, F7, F3, Fz, F4, and F8), temporal (T3, T4, T5, and T6), parietal (P3, Pz, and P4), central (C3, Cz, and C4), and occipital (O1 and O2).

The study utilized the reference montage method, with A1 and A2 as reference points. A referential montage EEG involves recording brain activity using electrodes placed on the scalp, with each electrode referenced to a common point, typically a neutral location such as the earlobe or mastoid. This method enhances the detection of localized brain activity by comparing the potential at each electrode to the common reference, thereby providing clearer insights into regional brain functions [20]. Figure 1 shows the setup of the EEG, including the position of each electrode, the mount used, and how this device is installed on the subject together with the head mounted display (HMD).

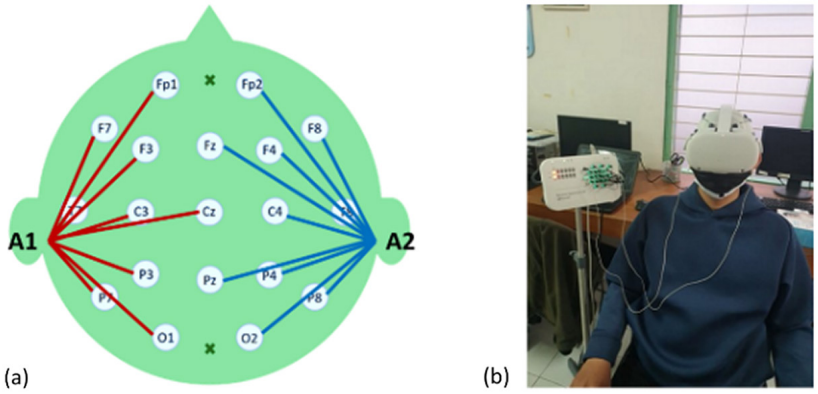

Fig. 1. Set up of the EEG device (a) referential montage (b) installation of the EEG and HMD on the participant

2.3 Data acquisition

This data acquisition explored the correlation between the EEG signals and the movement characteristics observed in the VR video. To ensure consistency, all VR videos were displayed using the HMD. The experiment consisted of two VR sessions, and the SSQ was administered four times to gauge the subjective assessment of VIMS both before and after the VR session, as indicated in Figure 2.

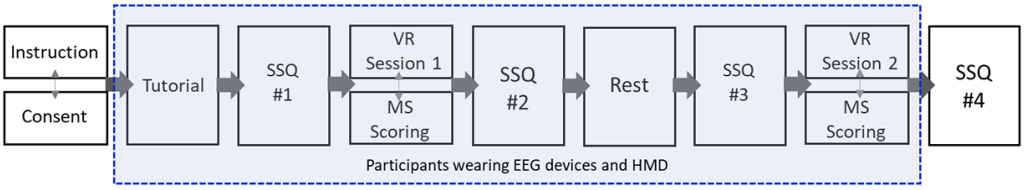

Fig. 2. EEG recording data acquisition workflow

Participants were asked to rate their motion sickness (MS) experience during both VR sessions, assessed during the intermission between sub-videos. The MS (MS) score was categorized into five levels: 0 (comfortable), 1 (mild sickness), 2 (moderate sickness), 3 (severe sickness), and 4 (extreme sickness). Figure 3. illustrates a group of participants being monitored using EEG, along with examples of multiple screenshots of the VR content.

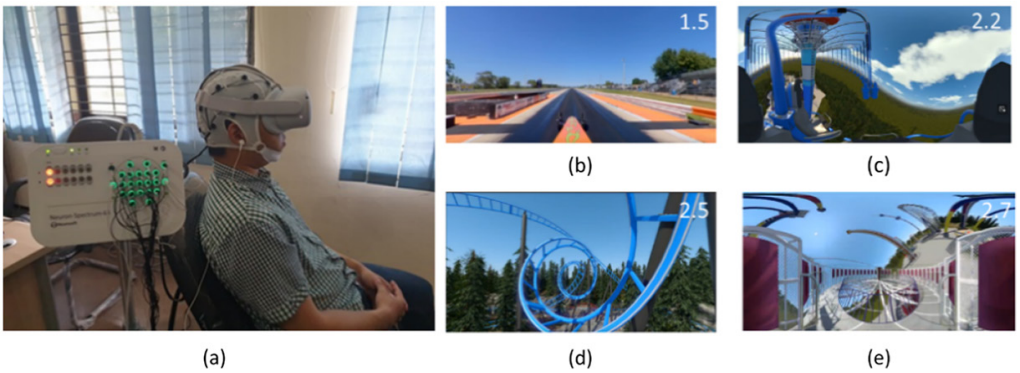

Fig. 3. Conditions for carrying out data acquisition (a) A participant is watching a VR show through an HMD while being measured using EEG (b)–(e) screenshots of several videos being shown

2.4 Virtual reality content and characterization of virtual motion parameters

During the initial virtual reality session, a video showcasing F1 car racing was presented, while in the subsequent VR session, a series of seven videos featuring different game rides were displayed. These videos were carefully selected to highlight various motion characteristics that may contribute to VIMS, such as circular and linear vection, bar and frame effects, and pseudo-Coriolis and Purkinje effects, among others [21].

Through the conducted experiments, it has been determined that the sensations felt by individuals when experiencing virtual reality can be categorized as either linear or circular motion.

Session 1 of the VR experience comprises five scene codes that exhibit motion in a two-dimensional plane. Each video scene lasts 20–40 seconds. In this particular session, the video depicts the viewpoint of a race car driver in a high-speed race setting. As illustrated in Figure 4, the diagram represents the motions observed in each of the five scene codes of VR Session 1 from the top view.

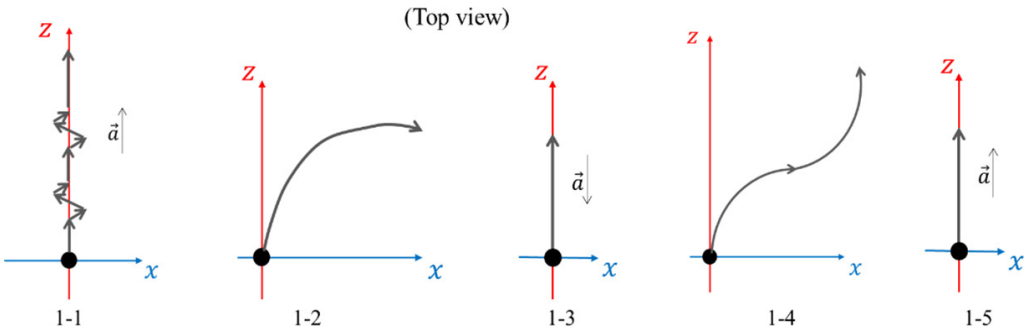

Fig. 4. Movement scheme for each video scene in session 1

The second VR session comprises seven scene codes showcasing movements in both horizontal and vertical planes. Each scene is captured in a 10- to 30-second video, offering a thrilling first-person perspective of various amusement park rides. Figure 5 illustrates the motion depicted in each scene code of VR Session 2.

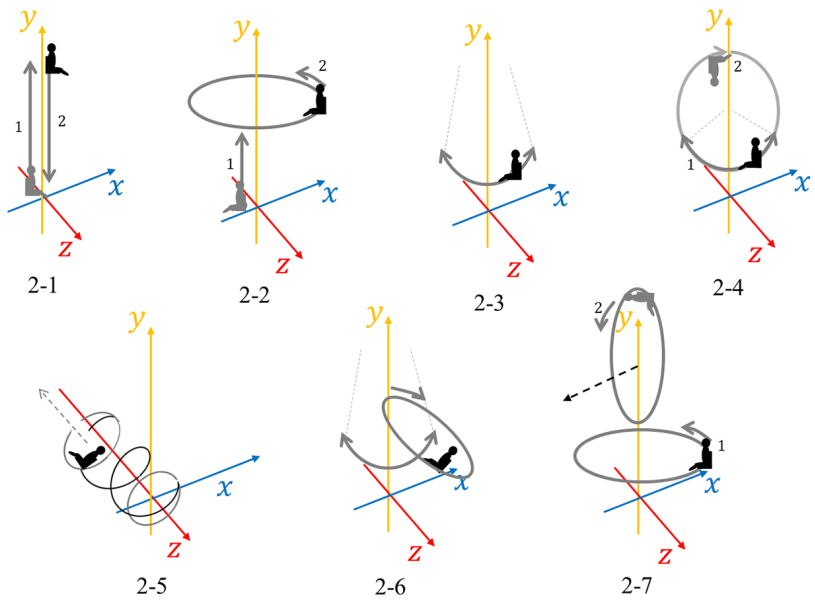

Fig. 5. Movement scheme for each video scene in session 2

2.5 Data processing

The EEG signal data is processed through multiple stages. Initially, the data is filtered to remove noise and artifacts. This is done using the bandpass filter (BPF) method, which transforms the signals from the time domain to the frequency domain using discrete Fourier transform (DFT) and then passes only the signals in the selected frequency range. The frequency range selected for this process is the brain wave frequency (0.5–100) Hz. The filtered data is then transformed into a time domain signal using inverse DFT. In the final stage of pre-processing, BPF is again used to pass the required signal frequencies, namely the frequency ranges of delta (δ) (0.5–4) Hz, theta (θ) (4–8) Hz, alpha (α) (8–13) Hz, beta (β) (13–30) Hz, and gamma (γ) (30–45) Hz [22].

Once the EEG signal is cleaned and separated based on brain wave frequency ranges, feature extraction is done through power spectral density (PSD). The PSD is then processed into several physical parameters that can be analyzed. Calculating the PSD of an EEG signal using Welch's periodogram method involves segmenting the EEG signal into overlapping sections, computing the periodogram for each segment, and then averaging these periodograms to obtain a smoother and less noisy PSD estimate. These steps help reduce the variance of the PSD estimate [23]. The signal is first segmented into overlapping sections, represented mathematically as

$$x_n(k) = x(k + nL) \tag{1}$$

where n is the segment index, k is the data point index within the segment, and L is the number of points by which segments overlap. For each segment, the periodogram is calculated using the equation

$$P_{xx}(f) = \frac{1}{N}\left|\sum_{n=0}^{N-1} w(n)x(n)e^{-j2\pi fn}\right|^2 \tag{2}$$

where $w(n)$ is the window function, and N is the segment length. Finally, the periodograms of all segments are averaged to obtain the PSD estimate described by

$$\hat{P}_{xx}(f) = \frac{1}{K}\sum_{k=0}^{K-1} P_{xx}^{(k)}(f) \tag{3}$$

where K is the number of segments and $P_{xx}^{(k)}(f)$ is the periodogram of the k-th segment. This approach results in a more stable and representative estimate of the frequency spectrum of the EEG signal.

This PSD calculation is carried out for the entire brain wave frequency range. Next, the power ratio calculation is carried out [24]. The beta/alpha ratio compares the PSD of beta to alpha-frequency brain waves. Apart from that, the theta/beta ratio compares the PSD of theta and beta-frequency brain waves [25].

3 RESULTS AND DISCUSSION

3.1 Simulator sickness questionnaire

The VIMS symptoms that participants experience can be described using the simulator sickness questionnaire (SSQ). In Figure 6, we can see the SSQ results calculated from 31 individuals. Four SSQ score calculations were conducted: before the VR show (SSQ#1), after session 1 of the VR show (SSQ#2), before session 2 of the VR show (SSQ#3), and after session 2 of the VR show (SSQ#4). A 15-minute break was provided between filling in SSQ#2 and SSQ#3 to allow the participant to return to their physical and mental state before engaging invirtual reality.

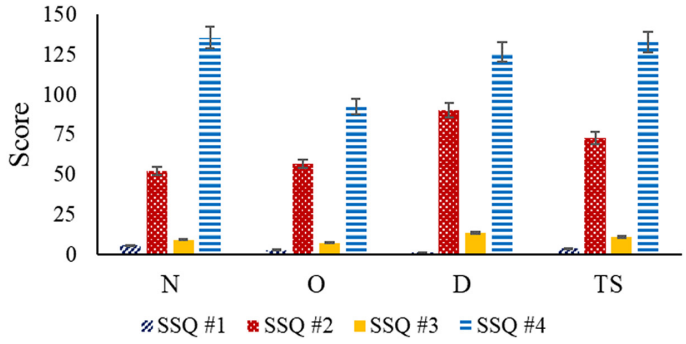

Fig. 6. SSQ results for four conditions during data acquisition (N, O, and D are symptom groups of nausea, oculomotor, and disorientation; while TS shows the total score)

Following participants' exposure to VR, significant improvements in all VIMS were observed, including reductions in nausea, oculomotor issues, and disorientation. In the first VR session, which featured car racing, the most notable improvement was seen in disorientation, with a score difference of 89.088. Nausea and dizziness were commonly experienced, regardless of whether participants had their eyes open or closed. Oculomotor symptoms showed a score increase of 53.818, involving general discomfort, fatigue, and eye strain. The nausea group also demonstrated a score increase of 46.746, primarily attributed to general discomfort and nausea. In the second VR session, set in an amusement park, the most significant improvement was observed in the nausea group, with a score change of 125.928. This change was commonly associated with general discomfort, nausea, and sweating. Disorientation

increased with a score of 112.752, predominantly due to nausea and dizziness. The oculomotor group reported an increase of 84.896, with general discomfort, fatigue, and eye strain as prevalent symptoms. Both VR sessions indicated overall positive changes in VIMS symptoms across all categories.

After analyzing the SSQ results, it was found that VR session 2 led to a greater increase in VIMS symptoms compared to VR session 1. This outcome is directly related to the content presented in each session. As previously discussed, VR session 2 incorporated more variations and levels of movement than VR session 1. The video footage was further categorized into 12 scene codes to facilitate a thorough comparison of the content in both VR sessions.

3.2 Motion sickness score

The MS score is a subjective measure used to quantify the severity of MS experienced by individuals. It is categorized into five distinct levels: 0 represents a state of comfort with no symptoms, 1 indicates mild sickness where symptoms are minimal and easily manageable, 2 denotes moderate sickness with more noticeable symptoms that may interfere with normal activities, 3 signifies severe sickness where symptoms are intense and significantly disruptive, and 4 corresponds to extreme sickness with overwhelming symptoms that can be incapacitating. This MS score will be used as a comparative aspect of the PSD value that will be obtained. The scores for each scene code were averaged to produce a final VR video scene score, presented in Table 1.

Table 1. Subjective score results for each VR video scene

VR Session 1		VR Session 2	
Scene Code	Average MS Score	Scene Code	Average MS Score
1–1	1.64 ± 0.642	2–1	2.17 ± 0.715
1–2	2.27 ± 0.686	2–2	1.08 ± 0.366
1–3	0.42 ± 0.409	2–3	2.44 ± 0.651
1–4	1.15 ± 0.385	2–4	3.31 ± 0.567
1–5	0.13 ± 0.343	2–5	3.80 ± 0.419
		2–6	3.93 ± 0.287
		2–7	2.67 ± 0.778

The motion complexity of each video scene varies, describing the number and sequence of movement types within it. For instance, scene code 2–2 features two motion characters appearing sequentially, while scene code 2–6 displays two motion characters occurring simultaneously. As a result, videos with scene code 2–6 are considered to have a higher level of complexity than those with scene code 2–2. Each code for a scene corresponds to a specific aspect of VIMS observed in VR videos, including linear vection, circular vection, uncertainty, pseudo-Coriolis, and Purkinje effects. These effects can be present independently or combined in a single scene. After each scene transition, participants were asked to rate their motion sickness level.

Upon analysis, it is apparent that videos featuring circular vection receive higher scores than those featuring linear vection. Additionally, videos with higher complexity are associated with higher scores than those with lower complexity. The video with the highest score involved scene code 2–6, which featured two types of

movement, oscillation and rotation, occurring simultaneously. This scene included circular vection and pseudo-Coriolis aspects. Conversely, videos with scene codes 1–5, which featured only one type of movement (accelerated straight movement), received the lowest scores. These videos only had one aspect, namely linear vection.

The scoring system is used to evaluate brain function by examining the correlation between motion sickness levels and physiological and neurological responses. For example, changes in brain activity measured by EEG can be studied in relation to the motion sickness score to gain insight into how different levels of motion sickness affect cognitive and neural processes. This approach helps pinpoint specific brain regions and neural pathways involved in the development and progression of motion sickness, offering valuable insights into the underlying mechanisms and potential treatment targets.

3.3 Power spectral density

The EEG recordings were analyzed to calculate the power spectral density (PSD) and compared with the participant's subjective assessments of motion sickness. The PSD values for each electrode within one group of brain regions were closely related. This was confirmed by the Wilcoxon test, which indicated that the average PSD value at electrodes in one brain region was not significantly different. It was observed that less than 5% of the pairs of electrodes in the frontal areas showed differentiation. Conversely, in other areas, there was no statistical distinction. Consequently, the PSD analysis represents an average of the PSD values for each channel within one brain area.

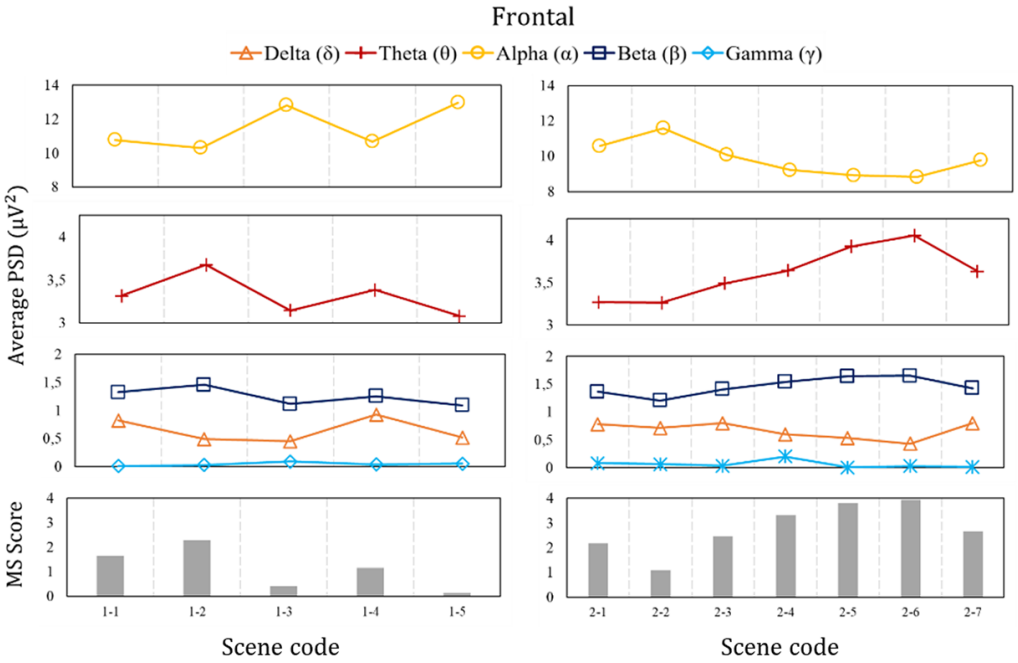

Fig. 7. Comparison of the average PSD of all brain waves in the frontal area (Fp1, Fp2, F7, F3, Fz, F4, and F8) to the motion characteristics of the video scene

Further, the average PSD value changes for each frequency range of brain waves are grouped according to the respective brain region. These changes are then compared with the score assigned to each scene code. The average PSD value for each video scene code in the frontal area and the participant's MS score are depicted in Figure 7. In both sessions, significant changes were noted in the alpha wave

frequency range, with the highest average PSD value (12.975 μV^2) recorded during scenes with the lowest score (0.13) and the lowest average PSD value (8.83 μV^2) during scenes with the highest score (3.93). Conversely, beta wave frequencies displayed an inverse relationship, where the average PSD values were directly proportional to the scene score. For example, scenes with the lowest score (0.13) corresponded to the lowest average PSD value (1.093 μV^2), while scenes with the highest score (3.39) exhibited the highest average PSD value (1.652 μV^2). It is worth noting that apart from these frontal alpha and beta wave frequencies, no other frequency ranges displayed significant changes throughout the analysis.

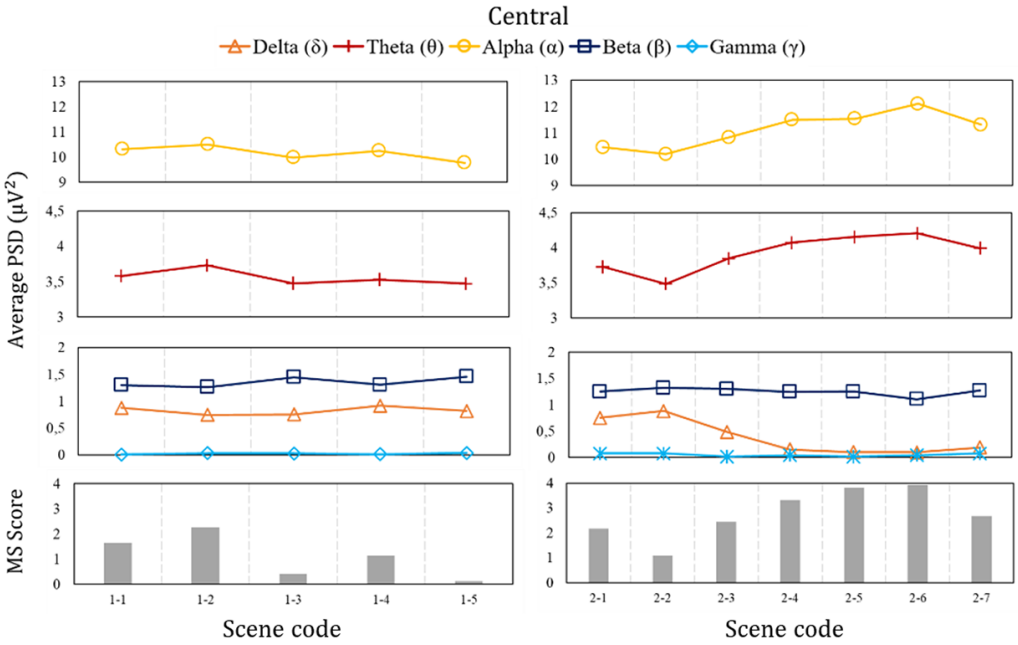

Fig. 8. Comparison of the average PSD of all brain waves in the central area (C3, Cz, and C4) to the motion characteristics of the video scene

As depicted in Figure 8, the central region displays notable variations in the theta frequency spectrum. Specifically, the theta wave frequency range undergoes substantial modifications correlating with the video scene transitions. Notably, the highest average PSD value (4.206 μV^2) corresponds to the scene with the highest score, while the lowest PSD value (3.4755 μV^2) aligns with the scene with the lowest score.

The frequency range of alpha waves in the central area shows the same pattern as theta waves. The average PSD value of the theta wave is directly proportional to the scene score. When the subject watched the video show with the lowest scene score (0.13), the average PSD value reached 9.78 μV^2. When the subject watched the video with the highest scene score (3.39), the average PSD value reached 12.105 μV^2. The beta wave frequency range in the central area experienced a significant change during VR session 1 but not in session 2.

Figure 9 shows the average PSD for the parietal area. The parietal area has three brain wave frequency ranges that experience significant changes during VR videos. It was observed that delta, theta, and alpha brain waves had significant changes in the average PSD values. The average PSD value in delta waves changes inversely to the scene score. Two representative points are the highest average PSD of 0.767 μV^2 and the lowest of 0.512 μV^2, which appeared when the subject saw the show with the highest and lowest scene scores, respectively.

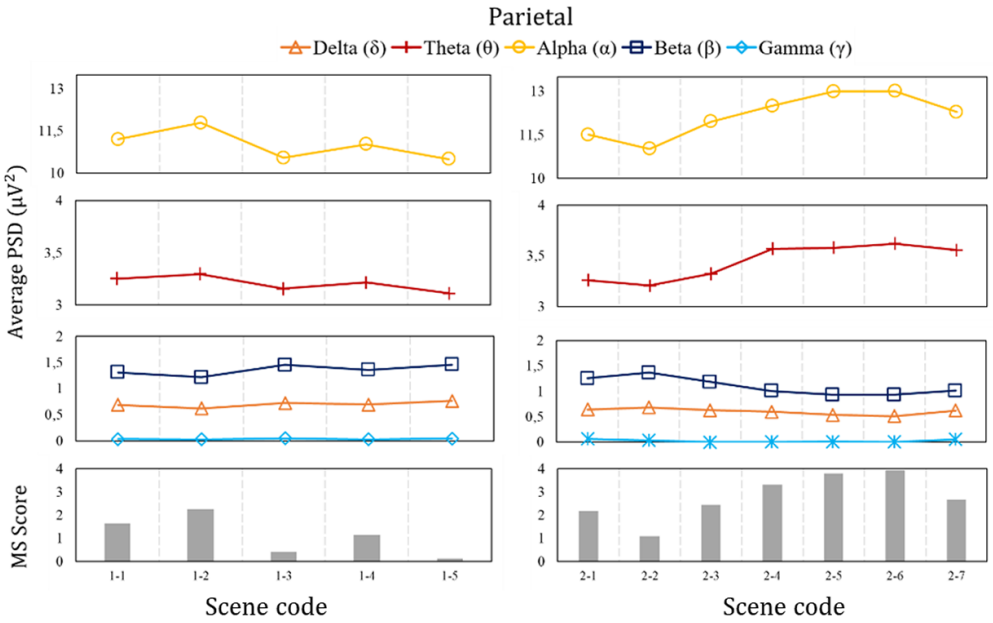

Fig. 9. Comparison of the average PSD of all brain waves in the parietal area (P3, Pz, and P4) to the motion characteristics of the video scene

On the other hand, theta and alpha waves exhibit a contrasting pattern to delta waves. The mean PSD values for theta and alpha waves are 3.6195 μV^2 and 13.01 μV^2, respectively. Notably, the subject displayed the highest average PSD value when viewing videos 2–6, which had the most captivating scenes. In contrast, the videos with the lowest scene score also had the lowest average PSD values for theta and alpha waves, namely 3.111 μV^2 and 10.4925 μV^2.

The mean PSD value did not significantly change in the temporal and occipital regions during VR video administration. In the temporal area, the theta wave frequency range only changed significantly during session 2. Meanwhile, in the occipital area, the delta wave changed significantly only in session 1 and the alpha wave only in session 2.

3.4 Relation of power spectral density to motion sickness score

After analyzing the PSD results, we focused on brain waves that exhibited notable changes. We then conducted a more in-depth analysis of the corresponding brain regions, including the frontal at alpha and beta frequencies, the central at alpha and theta frequencies, and the parietal at delta, theta, and alpha frequencies. To gain further insight, we utilized linear regression to investigate the relationship between the average PSD value and the scene score. Our analysis revealed two comparable results and five inverse relationships between the average PSD value and the scene score, depicted in Figure 10.

The observed changes in brain wave activity in response to VIMS can be justified by understanding the structural and biochemical dynamics of the brain regions involved. The inverse relationship between the average PSD value of alpha waves in the frontal area and the scene score suggests a functional modulation in response to sensory conflict and motion perception. Alpha waves, typically associated with a relaxed, wakeful state, show decreased activity as the brain's prefrontal

cortex adjusts to the perceived motion in a virtual environment. This adjustment reflects the prefrontal cortex's role in anticipating movement direction, where initial high activity diminishes as the frontal cortex processes and integrates sensory information, leading to an assumption of movement [26].

Conversely, the increase in beta wave activity in the frontal area during VIMS indicates heightened cognitive processing and mental workload. Beta waves are linked to active thinking, focus, and problem-solving, which aligns with the brain's need to resolve the sensory mismatch experienced during VIMS. This heightened activity can be attributed to increased neurotransmitter release, such as norepinephrine and dopamine, which are known to enhance alertness and cognitive functions during stress and sensory conflict [27], [28], [29], [30].

In the parietal area, which is responsible for processing body movement and sensory information, the direct relationship between the average PSD of alpha and beta waves and the severity of motion sickness highlights the role of the somatosensory system. The increased alpha and beta wave activity correlates with the brain's effort to reconcile conflicting sensory inputs from the visual and vestibular systems [31]. This sensory integration process involves complex neural circuitry and neurotransmitter interactions, such as the cholinergic and GABAergic systems, which modulate neural excitability and synaptic plasticity [32].

The central area's increased alpha and theta wave activity during heightened VIMS symptoms further supports the involvement of somatosensory processing. Theta waves are often associated with memory formation and navigation, suggesting that the brain is actively trying to contextualize and adapt to conflicting sensory information [33]. This process involves hippocampal and parahippocampal regions, which interact with the central somatosensory cortex to integrate sensory inputs and maintain spatial orientation. This finding aligns with prior study conducted by Krokos and Varshney [34], H. K. Lim et al. [30], and Nürnberger et al. [35].

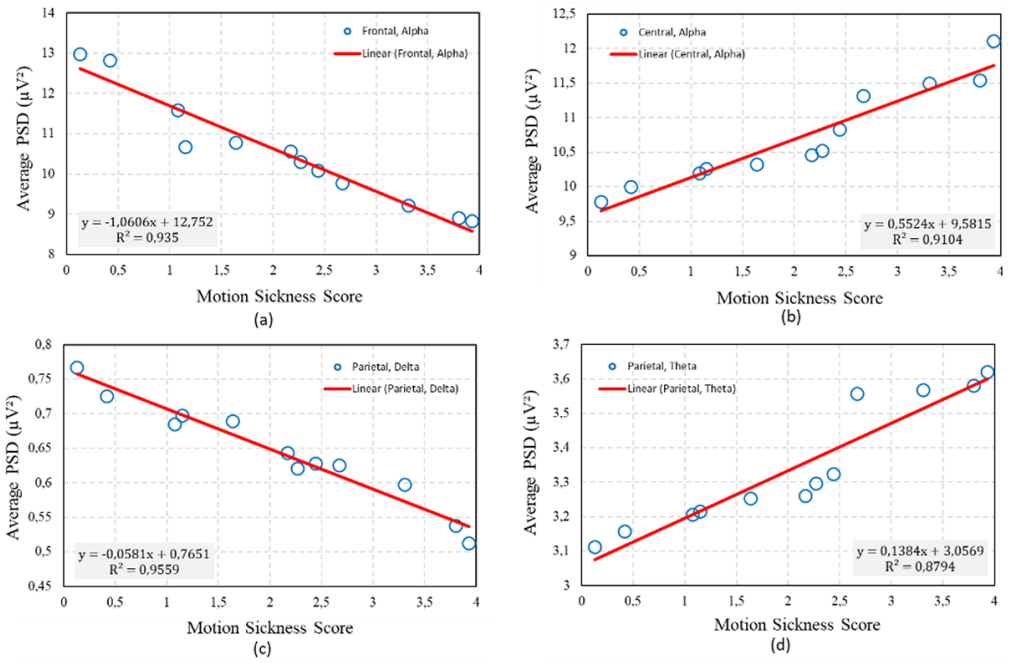

Fig. 10. *(Continued)*

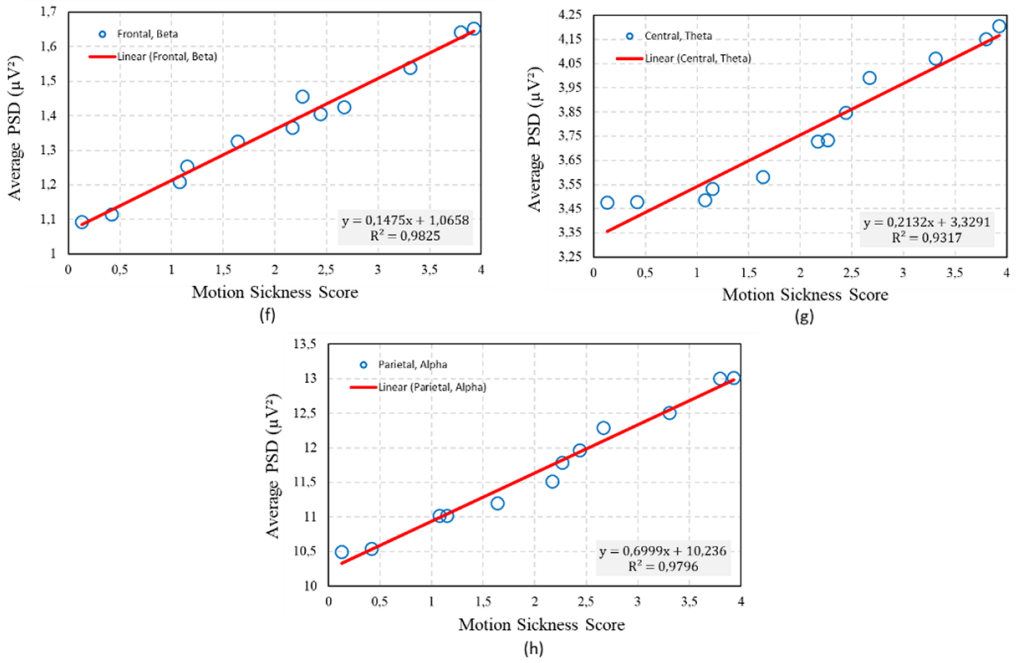

Fig. 10. The mean PSD values with significant changes were associated with MS scores via linear regression

3.5 Power ratio

A power ratio analysis was conducted to determine if the emergence of VIMS symptoms led to heightened cognitive load and stress levels. The results of the power ratio calculation are depicted in Figure 11, showcasing the beta/alpha ratio values as seen in Figure 11a. It is observed that the beta/alpha ratio value increases in tandem with the motion sickness score, which also escalates. These two data sets display a positive linear relationship with an R^2 score of 0.9834, implying that cognitive load intensifies as VR is introduced and the level of movement complexity surges [36], [37].

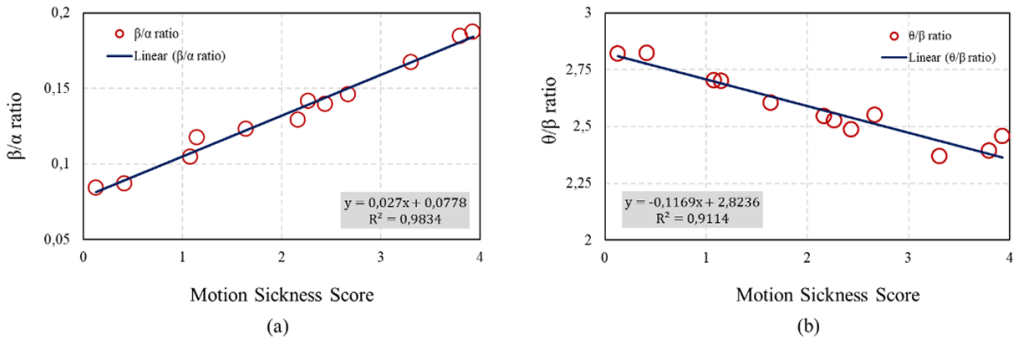

Fig. 11. Changes in the ratios (a) β/α and (b) θ/β are related to the score in each video scene

As observed in Figure 11b, the theta/beta ratio tends to have an inverse relationship with the motion sickness score. Linear regression analysis reveals that the two variables negatively correlate with a linear pattern. The obtained R^2 value of 0.9114 indicates a significant reduction in stress resistance levels. Therefore, it can be inferred that an increase in stress levels is also likely [38], [39].

4 CONCLUSIONS

This study study measured EEG activity in individuals exposed to VR content. The VR videos were thoughtfully selected to include variations in virtual motion parameters, considering factors that could potentially cause sensory conflict. The conclusions drawn from this study suggested that changes in the average PSD value were linked to the severity of VIMS symptoms, as determined by SSQ and motion sickness scoring. It is important to note that an increase in VIMS scores was strongly associated with significant changes in mean PSD. Furthermore, the study demonstrated that movement characteristics played a critical role in determining the level of VIMS experienced by participants. Specifically, more complex movements involving multiple types of motion simultaneously increased VIMS symptoms. Additionally, it was found that circular vection had a greater impact on VIMS than linear vection. The changes in brain wave activity during VIMS can be explained by the brain's structural and biochemical responses to sensory conflict. The modulation of alpha, beta, and theta waves across different brain regions reflects the complex interplay of neurotransmitter systems and neural circuits involved in sensory integration and cognitive processing during motion sickness. These findings could serve as preliminary data for developing an EEG signal-based VIMS detection system.

5 ACKNOWLEDGMENTS

We gratefully acknowledge the funding from the Institut Teknologi Bandung (ITB) research grant under the PPMI 2024 Program.

6 REFERENCES

[1] G. Al Farsi *et al.*, "A review of virtual reality applications in an educational domain," *International Journal of Interactive Mobile Technologies (iJIM)*, vol. 15, no. 22, p. 99, 2021. https://doi.org/10.3991/ijim.v15i22.25003

[2] D. K. Baroroh and A. Agarwal, "Immersive technologies in indonesia faces 'new normal' COVID-19," *International Journal of Technology*, vol. 13, 2022. https://doi.org/10.14716/ijtech.v13i3.5220

[3] R. P. Singh, M. Javaid, R. Kataria, M. Tyagi, A. Haleem, and R. Suman, "Significant applications of virtual reality for COVID-19 pandemic," *Diabetes & Metabolic Syndrome: Clinical Research & Reviews*, vol. 14, no. 4, pp. 661–664, 2020. https://doi.org/10.1016/j.dsx.2020.05.011

[4] R. S. Kennedy, J. Drexler, and R. C. Kennedy, "Research in visually induced motion sickness," *Appl Ergon*, vol. 41, no. 4, pp. 494–503, 2010. https://doi.org/10.1016/j.apergo.2009.11.006

[5] J. J. LaViola, "A discussion of cybersickness in virtual environments," *ACM SIGCHI Bulletin*, vol. 32, no. 1, pp. 47–56, 2000. https://doi.org/10.1145/333329.333344

[6] A. Jasper, N. Cone, C. Meusel, M. Curtis, M. C. Dorneich, and S. B. Gilbert, "Visually induced motion sickness susceptibility and recovery based on four mitigation techniques," *Front Virtual Real*, vol. 1, 2020. https://doi.org/10.3389/frvir.2020.582108

[7] N. S. Yahaya, A. A. Mutalib, and S. N. Abdul Salam, "A comparative analysis on cybersickness reduction guidelines in VR and IVR applications for children road safety education," *International Journal of Interactive Mobile Technologies (iJIM)*, vol. 16, no. 5, pp. 33–48, 2022. https://doi.org/10.3991/ijim.v16i05.26359

[8] J. T. Reason, "Motion sickness adaptation: A neural mismatch model," *J R Soc Med*, vol. 71, no. 11, pp. 819–829, 1978. https://doi.org/10.1177/014107687807101109

[9] A. S. Fernandes and S. K. Feiner, "Combating VR sickness through subtle dynamic field-of-view modification," in *2016 IEEE Symposium on 3D User Interfaces (3DUI)*, IEEE, 2016, pp. 201–210. https://doi.org/10.1109/3DUI.2016.7460053

[10] S. Sharples, S. Cobb, A. Moody, and J. R. Wilson, "Virtual reality induced symptoms and effects (VRISE): Comparison of head mounted display (HMD), desktop and projection display systems," *Displays*, vol. 29, no. 2, pp. 58–69, 2008. https://doi.org/10.1016/j.displa.2007.09.005

[11] J. E. Bos, W. Bles, and E. L. Groen, "A theory on visually induced motion sickness," *Displays*, vol. 29, no. 2, pp. 47–57, 2008. https://doi.org/10.1016/j.displa.2007.09.002

[12] P. Brown, P. Spronck, and W. Powell, "The simulator sickness questionnaire, and the erroneous zero baseline assumption," *Front. Virtual Real.*, vol. 3, 2022. https://doi.org/10.3389/frvir.2022.945800

[13] Y. S. Kim, J. Won, S.-W. Jang, and J. Ko, "Effects of cybersickness caused by head-mounted display–based virtual reality on physiological responses: Cross-sectional study," *JMIR Serious Games*, vol. 10, no. 4, p. 2022. https://doi.org/10.2196/37938

[14] E. Chang, M. Billinghurst, and B. Yoo, "Brain activity during cybersickness: A scoping review," *Virtual Real*, vol. 27, pp. 2073–2097, 2023. https://doi.org/10.1007/s10055-023-00795-y

[15] B. Keshavarz, K. Peck, S. Rezaei, and B. Taati, "Detecting and predicting visually induced motion sickness with physiological measures in combination with machine learning techniques," *International Journal of Psychophysiology*, vol. 176, pp. 14–26, 2022. https://doi.org/10.1016/j.ijpsycho.2022.03.006

[16] G. R. F. Suwandi, S. N. Khotimah, F. Haryanto, and Suprijadi, "Electroencephalography signal analysis for virtual reality sickness: Head-mounted display and screen-based," *International Journal on Advanced Science Engineering Information Technology*, vol. 13, 2023. https://doi.org/10.18517/ijaseit.13.4.18165

[17] D. Weber *et al.*, "A structured approach to test the signal quality of electroencephalography measurements during use of head-mounted displays for virtual reality applications," *Front. Neurosci.*, vol. 15, 2021. https://doi.org/10.3389/fnins.2021.733673

[18] E. Ugur, B. O. Konukseven, M. Topdag, M. E. Cakmakci, and D. O. Topdag, "Expansion to the motion sickness susceptibility questionnaire-short form: A cross-sectional study," *J. Audiol. Otol.*, vol. 26, no. 2, pp. 76–82, 2022. https://doi.org/10.7874/jao.2021.00577

[19] World Medical Association, "World medical association declaration of Helsinki," *JAMA*, 2013. https://doi.org/10.1001/jama.2013.281053

[20] G. R. F. Suwandi, S. A. Risyad, S. N. Khotimah, F. Haryanto, and S. Suprijadi, "A comparative study of alpha frequency analysis between medical and consumer-grade electroencephalography devices on the measurement of male healthy subjects," *Malaysian Journal of Fundamental and Applied Sciences*, vol. 19, 2023. https://doi.org/10.11113/mjfas.v19n6.3156

[21] R. Lewkowicz, "Modeling motion sickness," *The Polish Journal of Aviation Medicine, Bioengineering and Psychology*, vol. 22, no. 3, 2017. https://doi.org/10.13174/pjambp.12.07.2017.04

[22] T. Najafi, R. Jaafar, R. Remli, W. A. Wan Zaidi, and K. Chellappan, "Brain dynamics in response to intermittent photic stimulation in epilepsy," *International Journal of Online and Biomedical Engineering (iJOE)*, vol. 18, pp. 80–95, 2022. https://doi.org/10.3991/ijoe.v18i05.27647

[23] G. R. F. Suwandi, S. N. Khotimah, and Suprijadi, "Electroencephalography signal power spectral density from measurements in room with and without faraday cage: A comparative study," in *J. Phys. Conf. Ser.*, 2022, vol. 2243. https://doi.org/10.1088/1742-6596/2243/1/012002

[24] Q. Xiong, X. Zhang, W.-F. Wang, and Y. Gu, "A parallel algorithm framework for feature extraction of EEG signals on MPI," *Comput Math Methods Med*, vol. 2020, pp. 1–10, 2020. https://doi.org/10.1155/2020/9812019

[25] T. Yi Wen and S. A. Mohd Aris, "Electroencephalogram (EEG) stress analysis on alpha/beta ratio and theta/beta ratio," *Indonesian Journal of Electrical Engineering and Computer Science*, vol. 17, 2020. https://doi.org/10.11591/ijeecs.v17.i1.pp175-182

[26] B. Ren, W. Guan, and Q. Zhou, "Study of motion sickness model based on fNIRS multi-band features during car rides," *Diagnostics*, vol. 13, no. 8, 2023. https://doi.org/10.3390/diagnostics13081462

[27] C. A. T. Cortes, C.-T. Lin, T.-T. N. Do, and H.-T. Chen, "An EEG-based experiment on VR sickness and postural instability while walking in virtual environments," in *2023 IEEE Conference Virtual Reality and 3D User Interfaces (VR)*, 2023, pp. 94–104. https://doi.org/10.1109/VR55154.2023.00025

[28] Y.-C. Chen *et al.*, "Spatial and temporal EEG dynamics of motion sickness," *Neuroimage*, vol. 49, no. 3, pp. 2862–2870, 2010. https://doi.org/10.1016/j.neuroimage.2009.10.005

[29] K.-M. Jang, M. Kwon, S. G. Nam, D. Kim, and H. K. Lim, "Estimating objective (EEG) and subjective (SSQ) cybersickness in people with susceptibility to motion sickness," *Appl. Ergon.*, vol. 102, 2022. https://doi.org/10.1016/j.apergo.2022.103731

[30] H. K. Lim *et al.*, "Test-retest reliability of the virtual reality sickness evaluation using electroencephalography (EEG)," *Neurosci. Lett.*, vol. 743, 2021. https://doi.org/10.1016/j.neulet.2020.135589

[31] C.-T. Lin, S.-W. Chuang, Y.-C. Chen, L.-W. Ko, S.-F. Liang, and T.-P. Jung, "EEG effects of motion sickness induced in a dynamic virtual reality environment," in *29th Annual International Conference of the IEEE Engineering in Medicine and Biology Society*, 2007, pp. 3872–3875. https://doi.org/10.1109/IEMBS.2007.4353178

[32] Q. Gu, "Neuromodulatory transmitter systems in the cortex and their role in cortical plasticity," *Neuroscience*, vol. 111, no. 4, pp. 815–835, 2002. https://doi.org/10.1016/S0306-4522(02)00026-X

[33] G. Buzsáki, "Theta oscillations in the hippocampus," *Neuron*, vol. 33, no. 3, pp. 325–340, 2002. https://doi.org/10.1016/S0896-6273(02)00586-X

[34] E. Krokos and A. Varshney, "Quantifying VR cybersickness using EEG," *Virtual Real*, vol. 26, pp. 77–89, 2022. https://doi.org/10.1007/s10055-021-00517-2

[35] M. Nürnberger, C. Klingner, O. W. Witte, and S. Brodoehl, "Mismatch of visual-vestibular information in virtual reality: Is motion sickness part of the brains attempt to reduce the prediction error?" *Front. Hum. Neurosci.*, vol. 15, 2021. https://doi.org/10.3389/fnhum.2021.757735

[36] N. Schaworonkow, "Overcoming harmonic hurdles: Genuine beta-band rhythms vs. contributions of alpha-band waveform shape," *Imaging Neuroscience*, 2023. https://doi.org/10.1162/imag_a_00018

[37] B. J. Griffiths *et al.*, "Alpha/beta power decreases track the fidelity of stimulus-specific information," *Elife*, vol. 8, 2019. https://doi.org/10.7554/eLife.49562

[38] T. H. Priya, P. Mahalakshmi, V. Naidu, and M. Srinivas, "Stress detection from EEG using power ratio," in *2020 International Conference on Emerging Trends in Information Technology and Engineering (ic-ETITE)*, 2020, pp. 1–6. https://doi.org/10.1109/ic-ETITE47903.2020.401

[39] A. Angelidis, W. van der Does, L. Schakel, and P. Putman, "Frontal EEG theta/beta ratio as an electrophysiological marker for attentional control and its test-retest reliability," *Biological. Psychol.*, vol. 121, pp. 49–52, 2016. https://doi.org/10.1016/j.biopsycho.2016.09.008

7 AUTHORS

Galih Restu Fardian Suwandi is an Assistant Professor at the Faculty of Mathematics and Natural Sciences, Institut Teknologi Bandung. His research interests encompass biophysics, neuroscience, and medical physics. With broad expertise in these interdisciplinary fields, he dedicates himself to advancing our comprehension of biological systems and medical technologies, focusing on the intersection between physical principles and biomedical applications (E-mail: galihrfs@itb.ac.id).

Siti Nurul Khotimah is a Professor of Charged Particle Dynamics Physics at the Faculty of Mathematics and Natural Sciences, Institut Teknologi Bandung. Her research interests span biophysics, electrophysiology, statistical physics, and charged particle dynamics. Armed with an in-depth understanding of these areas, she is committed to advancing theoretical and applied physics knowledge, specifically focusing on the dynamics of charged particles and their implications in biophysical and electrophysiological contexts (E-mail: nurul@itb.ac.id).

Freddy Haryanto, an Associate Professor at the Faculty of Mathematics and Natural Sciences, Institut Teknologi Bandung, directs his research interests toward medical physics. He explores the convergence of physics and medical applications to improve diagnostic and therapeutic technologies. Committed to advancing medical science, his research enhances healthcare outcomes by implementing innovative physical methods and technologies (E-mail: freddy@itb.ac.id).

Suprijadi, a Professor of Computational Science and Material Properties Characterization at the Faculty of Mathematics and Natural Sciences, Institut Teknologi Bandung, focuses on instrumentation physics, computational physics, and material characterization. With substantial expertise in these areas, his work advances the understanding of material properties through computational methods and innovative instrumentation, making significant contributions to physics and materials science (E-mail: suprijadi@itb.ac.id).